

Finding Very Small Near-Earth Asteroids using Synthetic Tracking

Michael Shao, Bijan Nemati, Chengxing Zhai, Slava G. Turyshev, Jagmit Sandhu
*Jet Propulsion Laboratory, California Institute of Technology,
 4800 Oak Grove Drive, Pasadena, CA 91109-0899, USA*

Gregg W. Hallinan, Leon K. Harding
California Institute of Technology, 1200 E. California Blvd., Pasadena 91125, USA
 (Dated: July 29, 2018)

We present a new technique that is designed to significantly increase the sensitivity for finding and tracking small and fast moving near Earth asteroids (NEAs). The technique relies on a combined use of a novel data processing approach and a new generation of high-speed cameras which allow taking short exposures of moving objects at high frame rates, effectively “freezing” their motion. Although the signal to noise ratio (SNR) of a single short exposure is insufficient to detect the dim object in one frame, by shifting successive frames relative to each other and then co-adding the shifted frames in post-processing, we synthetically create a long-exposure image as if the telescope were tracking the object with a significantly higher SNR. We call this approach “synthetic tracking.” In addition to the enhancement of the SNR for asteroid detection, synthetic tracking also improves the astrometric accuracy of the detected objects relative to background stars. We apply this technique to observations of two known asteroids conducted on the Palomar 200-inch telescope and demonstrate the improved SNR and the 10-fold improvement of astrometric precision over the traditional long exposure approach. In the past 6 years, about 150 of NEAs with absolute magnitudes $H=28$ mag (~ 10 m in size) or fainter have been discovered. With an upgraded version of our camera and a field of view of $(28 \text{ arcmin})^2$ on the Palomar 200-inch telescope, synthetic tracking could allow detecting of up to 80 such objects per night including very small NEAs, with sizes down to 7 m.

I. INTRODUCTION

Studies of near-Earth asteroids (NEAs) have a significant value for scientific discovery, as they are believed to be remnants from the early evolution of the solar system. Accordingly, information about NEA composition and chemical properties provide important clues about conditions present during that early epoch. However, near-Earth objects also present a threat to life on Earth, as some of them may come close to and even impact the Earth. Notable examples include the Tunguska event over Eastern Siberia in June 1908, the recent atmospheric entry of a 17 m asteroid followed by a fireball over the city of Chelyabinsk in Russia on Feb. 15, 2013, and, on the same day, the flyby of a 50 m sized asteroid that passed closer to Earth than the orbits of geosynchronous satellites. In fact, a few times each year, an object of the size of a small car hits Earth’s atmosphere. When these burn up on their descent through the atmosphere, they leave a beautiful trail of light known as a meteor or “shooting star.” Larger asteroids occasionally crash into Earth, creating craters, such as Arizona’s kilometer-wide Meteor Crater near Flagstaff. Another impact site off the coast of the Yucatan Peninsula in Mexico, which is buried by ocean sediments today, is believed to be a record of the event that led to the extinction of the dinosaurs some 65 million years ago. Fortunately, these big asteroid impacts are rare.

While there has been a long history of NEA studies, the reasons above have led to recently intensified interest in the discovery and characterization of NEAs resulting in multiple currently ongoing worldwide efforts to search and catalog their population [7, 9]. Two of the most productive search programs are the Panoramic Survey Telescope and Rapid Response System (Pan-STARRS)¹ on Maui, Hawaii, and the Catalina Sky Survey (CSS)² in Tucson, Arizona. To date over 10,000 NEAs have been discovered, with nearly 1,000 of these objects being over 1 km in size. In fact, the current techniques for discovering NEAs either from space or the ground have been highly successful in detecting bodies larger than 1 km.

While great strides are being made, the completeness of the known asteroid population drops rapidly for significantly smaller NEAs. In particular, the existing population of near Earth asteroids smaller than 50 m is largely under-explored [10]. To date, only a small number of NEAs with sizes of 50 m have been discovered, but the vast majority, as much as 98%, of the estimated half a million 50 meter-class NEAs have not yet been found [8]. Moreover, of those found, most are subsequently lost because their orbits cannot be determined with sufficient accuracy.

¹ The Panoramic Survey Telescope and Rapid Response System (Pan-STARRS): <http://pan-starrs.ifa.hawaii.edu/>

² The Catalina Sky Survey (CSS): <http://www.lpl.arizona.edu/css/>

Recognizing the importance of finding NEAs, NASA recently announced the Asteroid Grand Challenge³, which aims to detect all NEAs – including those less than 10 meters in size that are in retrievable orbits – determining their orbits, and characterizing their shape, rotation state, mass, and composition as accurately as possible. The objectives include both planetary protection and the identification of possible human spaceflight targets for a proposed Asteroid Redirect Mission (ARM). The latter includes small NEAs with sizes 7–10 m in low delta-velocity orbits with respect to the Earth.

Observing NEAs is quite different from observing the objects outside the solar system. Part of the problem is the fact that all NEAs move, even during relatively short, 30 sec exposures. In addition, small NEAs are dim (absolute magnitudes in the range $H \sim 28$ –30) and thus are observable only when they are already close to the Earth (closer than 0.1 AU). However, in that situation, the NEA is also moving very fast across the sky, with proper motion of several degrees per day ($^\circ/\text{day}$). NASA’s Jet Propulsion Laboratory (JPL) maintains a website⁴ that lists the expected upcoming ~ 100 encounters with NEAs. The average velocity of these objects is ~ 10 km/s relative to the Earth, which, at the distance of 0.1 AU, results in apparent proper motion of 0.14 arcsec per second ($''/\text{sec}$). Under $1''$ seeing conditions (typical at the Palomar 200 in telescope), an exposure longer than 7 sec of the average object would result in a streaked image. Thus, traditional surveys of NEAs, with exposures of 30 seconds or more, have significantly lower sensitivity for fast moving NEAs as compared to slowly moving ones. As a result, finding and tracking of small (5–10 m in size), dim ($H \sim 28$ –30 in absolute magnitude), and fast moving NEAs (few $^\circ/\text{day}$ in proper motion) is a major challenge.

Nearly all of the very smallest $H \sim 28$ –30 NEAs that are discovered are subsequently lost.⁵ The very smallest NEAs are detectable for only a week; at other times they are too faint to be detected. If the astrometry data collected during that week is not sufficiently accurate to predict the position of the asteroid 4–6 years in the future when it next comes close to Earth; the object is lost. This, we believe, is the great challenge in small NEA investigations at this time. Without the ability to track the NEAs after their first discovery, creating a catalog and census of these objects becomes very difficult. Similarly, planetary protection interests in these investigations require that they are not lost after initial discovery.

In this paper, we describe a new technique, called “synthetic tracking,” that can find very small NEAs with brightness down to $H=30$. We then show how synthetic tracking allows much improved astrometry, so that discovered objects can subsequently be tracked with enough precision to avoid being lost in the future. Section 2 presents the details of the method along with a discussion of its performance relative to traditional methods. In Section 3, we report on test observations we made on two asteroids using the Palomar 200-inch (5.1 m) telescope on April 3, 2013 with a high-speed, low noise camera. Section 4 provides a closer look of the detection aspect, and the implications on the design of the major components of a next-generation small-NEA detection instrument. Section 5 focuses on the important errors affecting astrometry, and how they are mitigated. Section 6 is a summary with conclusions.

II. BACKGROUND

To detect a dim object, it is important to observe the object long enough to accumulate the necessary number of photons. The current approach to observe NEAs is to use 30-second exposures.⁶ Long exposure is necessary to avoid the excessive read noise associated with reading out each of the camera frames. Subsequent follow up images of the same field are then recorded about an hour later and the two images ‘blinked’ to detect moving objects.

Since small NEAs become detectable only when they are close to Earth, they typically move very fast (a few $^\circ/\text{day}$ or $\sim 10''/\text{min}$) in the field. During the observable period, a long (e.g. 30 sec) exposure of such an object leaves a streak on the charged couple device (CCD) that covers many pixels (often several arcseconds long) instead of a single spot. The streaked image has two disadvantages: 1) it includes more noise from the background as it covers a larger area on the CCD; 2) the streaked shape depends on the atmospheric motion during the integration period and cannot easily be compared with a reference star in the field, leading to large errors in astrometry [13]. Poor orbits means they will likely be lost by the time the next encounter occurs; they will be mistaken as new discoveries.

Small (10 meter-class) NEAs are very faint. Such objects are detectable only when they are very close to the Earth, and hence moving rapidly across the sky. We simulated a 10 m NEA of $H=28$ mag as it approaches the Earth with an impact parameter of 1 lunar distance (LD). This is shown in Fig. 1. The NEA is moving parallel to the Earth’s

³ The NASA Asteroid Grand Challenge: http://www.nasa.gov/mission_pages/asteroids/initiative/index.html

⁴ The Near Earth Objects Program’s website at JPL: <http://neo.jpl.nasa.gov/>

⁵ At the “Target NEO 2” workshop held on July 9, 2013, the director of the SAO Minor Planet Center was asked the question, “What fraction of the very smallest $H \sim 28$ –30 NEAs that are discovered are subsequently lost?” The answer was “almost all of them.”

⁶ Pan-STARRS, for example, uses a 30 sec exposure time.

orbit around the Sun but moving 2.5 km/s faster (or slower) than the Earth. The simulation includes the phase angle effect assuming a spherical NEA and assumes Lambertian reflectance of sunlight. From this set of assumptions, we plot a number of quantities in Figure 2: the distance from the NEA to the Earth, the on-sky velocity, the apparent magnitude, and the apparent magnitude scaled to a 30 sec CCD exposure. This last quantity represents the loss of SNR due to the streaking of the image, and is computed using Eq. (1). The streak-corrected sensitivity assumes the detection is based on the peak flux in a $1''$ box (the assumed seeing limit) in the streaked image.

Many telescopes of different sizes are used to conduct search for NEAs. If we assume that a telescope has sufficient sensitivity to detect (at a good SNR) a stationary 21-mag star, then, at 17 days before the closest encounter, this $H=28$ mag object would have an apparent mag of 21. However, at 17 days, the on-sky motion would be slightly more than $3.5^\circ/\text{day}$, streaking the image so the brightness of the streak is the same as a 22.8-mag star (Fig. 2). By the time the brightness of the streaked image was brighter than 21 mag, at 5 days before closest encounter, the velocity is over $10^\circ/\text{day}$. Instead of being detectable for only 10 days during this encounter, synthetic tracking with the same telescope could detect this object 34 days prior to the close encounter.

One can estimate the loss of sensitivity from a streaked image. Many NEA searches start with two images of the same part of the sky taken roughly 15 min apart. The difference of the two images will remove the stationary objects, the stars. The NEA shows up as a positive blip in the first exposure and a negative blip in the second one that is subtracted. A common approach is to set the discovery threshold at 5σ , that is, a detection signal-to-noise ratio (SNR) of 5. Detection SNR is used to assess the false alarm rate and is given by the ratio of the signal over the noise from only the background. If the signal from the object is above the threshold, one could claim a detection. To avoid too many false alarms, a third image is often taken. The velocity of the object must be consistent between the three images for the detection to be valid. The set of three or more images is called a ‘tracklet’ [6]. If the focal plane has pixels that are smaller than the point spread function (PSF), instead of comparing each pixel against a threshold, one would perform a low pass spatial filter analysis of the image before subjecting it to a threshold. The low pass filter integrates the signal under the PSF. For reference, we will call this the ‘basic technique.’

III. SYNTHETIC TRACKING APPROACH

A solution to the trailing loss for fast moving objects is to use shorter exposure times such that the streak in each image is no worse than the typical $1''$ seeing limit. For an object moving at $\sim 20^\circ/\text{day}$ (or $\sim 1''/\text{sec}$), this suggests an exposure time of 1 sec, i.e. 1 frames per second (fps) frame rate. However, this exposure is not long enough to see faint objects. Hence, a series of exposures have to be taken, so that, when the images are subsequently shifted and added, the resultant SNR is that of a long (e.g. 30-sec) exposure. The major obstacle in this approach has been the fact that not only the traditional large format CCDs cannot be read-out at such a high rate; they would also have a prohibitively high read-noise when run at such frame rates.

Our approach to detecting small NEAs relies on using a new type of high-speed ultra-low noise commercial-off-the-shelf (COTS) cameras originally designed for the medical imaging. These are ~ 4 – 5 megapixel (Mpix) cameras that can take up to 100 frames/sec with only $1e^-$ read noise. They represent a newer generation of CMOS technology,

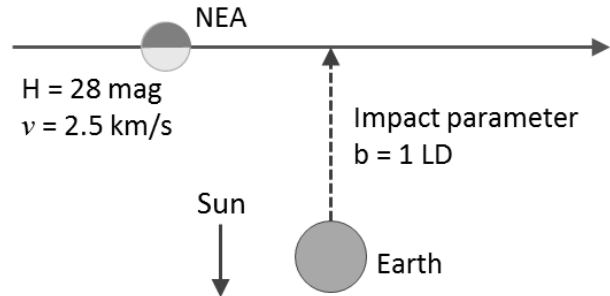


FIG. 1: Geometry of a simulated Earth flyby of a small, dim, and fast-moving NEA.

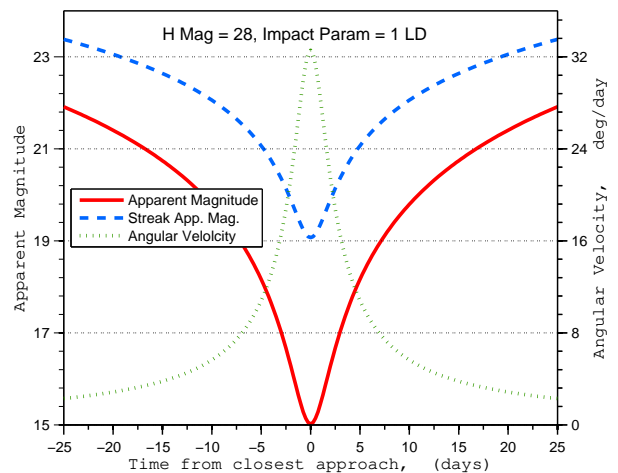


FIG. 2: Results of the simulated flyby shown in Fig. 1. The angular velocity and apparent magnitude (with and without loss due to streaking) are shown.

called Scientific CMOS (sCMOS), which enables fast frame-rate imaging. One excellent representative of this class (the AndorTM Zyla⁷) features small pixel size ($6.5\ \mu\text{m}$), high resolution (2560×2160), good dynamic range (16 bits), high frame rate ($\sim 100\ \text{Hz}$), and very importantly, low read-out noise ($1.2\ e^-$). Such a camera is well suited to the challenge of detecting faint NEAs. At a frame rate of 2 fps the read noise of the camera is lower than the zodiacal (zodi) background, thus not paying much penalty from fast reading.

In the post-processing, we can shift and add these short exposure frames according to the appropriate velocity of the NEA to synthesize a long exposure, equivalent to the telescope tracking on the target. We illustrate the basic idea in Fig. 3, where the vertical layers correspond to successive camera frames. Because the target moves in the field, its location in each frame is different. If we know the velocity of the NEA in advance, we can then shift the frames relative to each other according to this velocity so that the location of the NEA is kept constant with respect to the first frame. Successive images are shifted before being added. If the shift vector matches the asteroid on-sky velocity, the asteroid photons will add and the noise from the zodi background will be limited to the seeing limited PSF. As we add all the images along the vertical line (synthetic long exposure), the signal of the NEA increases linearly with the number of frames while the noise goes as the square root of the number of frames, thus SNR increases as the square root of the number of frames. With a sufficient number of frames, the NEA signal will exceed the noise from the zodi background.

As an example, consider an NEA that moves at $0.2''/\text{sec}$ on the sky, observed with a photon rate of 5 photons/sec, against a zodi background of 4 photons/arcsec²/sec. Assuming $1''$ seeing, in a conventional, 30-sec CCD exposure, 150 photons from the NEA would be detected spreading across a ($1'' \times 6''$) streak. Each 1 arcsec² area would have only 25 NEA photons and 120 zodi photons. The SNR of interest here is the detection SNR. Thus the surface brightness of the streak would have a detection SNR of $25/\sqrt{20} \simeq 2.3$. This is too small to be called a detection. In synthetic tracking using currently available sCMOS cameras, the observation is broken into 1 sec exposures with a camera that has $\sim 1\ e^-$ of noise and 60% quantum efficiency (QE). The zodi noise in each frame adds in quadrature with the $\sim 1\ e^-$ of read noise. The synthetically composed image thus has 90 signal electrons, while the variance of the background is $72\ e^-$ from zodi plus $30\ e^-$ from read noise. The detection SNR for synthetic tracking is $90/\sqrt{72 + 30} \simeq 8.9$, approximately the same as that of the seeing limited PSF. This improvement in the SNR is similar to that reported using a matched filter technique [4].

Our technique works efficiently on detecting small and fast NEAs because the improvement of SNR by using synthetic tracking is proportional to the velocity of the asteroid in the sky. A traditional survey uses a ‘tracklet’ (e.g. two, 30 sec exposures at 1 fps, 15 min apart) to detect NEAs. Our analogous tracklet would be 60 images collected over 30 sec followed by an additional 60 images 15 min later. The 120 images would be analyzed as a single data set fitting the position and velocity of the object. The separation into ‘epochs’ that are tens of minutes apart improves our efficiency for slow moving objects. For example, in a single, 30 sec epoch, objects with motion less than $1''$ per 30 sec would look stationary and not discernible from background stars. For most NEAs, requiring the motion within 30 sec to match the motion between 2 observations 15 min apart might be sufficient to claim a ‘discovery.’ In the near future and once more data is collected, we will examine instrumental artifacts and evaluate contributing of various noise sources. This would allow us to conduct a thorough analysis of false alarms anticipated with the synthetic tracking technique.

Before the detection of the NEA, its velocity vector is unknown. However, we find this vector by conducting a search in velocity space. To do this we have developed an algorithm that simultaneously processes the synthetic tracking data at different velocities. The velocities searched initially have (x,y) components that are multiples of 1 pix/frame in each direction. This is a computationally intensive task: for example, the shift and add process for 120 images for 1,000 different velocity vectors requires over 10^{11} arithmetic operations. However, with current off-the-shelf graphics processing units (GPU) with up to 2,500 processors and teraFLOPS peak speeds, we were able to analyze 30 sec of

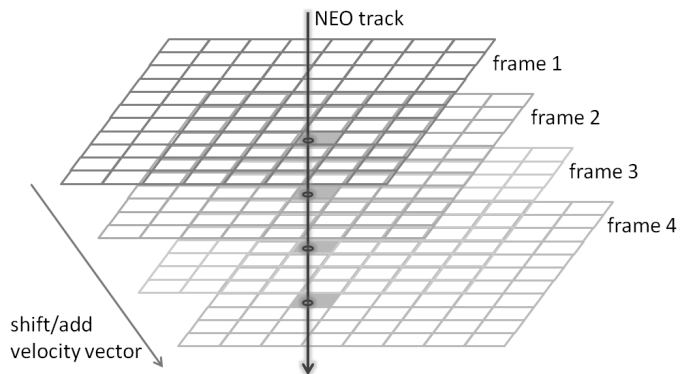


FIG. 3: Shift-and-add concept illustrated: because of the motion of the NEA, photons are deposited on different pixels of a CCD, but in the synthetic image (with shifted/added frames) the asteroid smear is removed.

⁷ For description of the AndorTM Zyla camera, see http://www.andor.com/pdfs/literature/Andor_sCMOS_Brochure.pdf

data in less than 10 sec. Once the NEA is detected in this initial search, an estimate of velocity becomes possible. Using this velocity we refine the astrometry relative to a reference star in the field and determine the velocity to a much higher precision. Elsewhere we plan to describe the details of the synthetic tracking algorithm and report its performance, including its false alarm rate.

IV. THEORETICAL COMPARISON OF METHODS FOR DETECTION SNR

In the ‘basic technique’ described above, a streaked image spreads the light across more pixels reducing the signal and SNR. This effect is known as ‘trailing loss’ and its magnitude is given by the factor:

$$\epsilon_t = \frac{w}{w + s}, \quad (1)$$

where w is the width of a stellar image and s is the length of the streak. If an object is streaked, the photons from that object are spread over a larger number of pixels. The background, in the meanwhile, is constant.

If a telescope has a magnitude limit of 21 mag, a fast moving asteroid with an absolute magnitude of $H=26$ would not be detectable at distances over 0.1 AU from the Earth. However, even at distances of 0.1 AU or closer, it would be detectable only if the streak were shorter than the width of the stellar image (i.e. if the streak did not significantly affect the SNR). The main difference between 10-m class asteroids and 100-m class asteroids is that the latter are detectable much farther from the Earth and, on average, they will move 10 times slower.

Figure 4 shows the reduction in the distance needed to detect an asteroid when it moves at 2.5 km/s or 9.5 km/s with respect to the Earth. We assume the sensitivity limit of ~ 21 mag for a 1-m telescope and 30 sec integration. An $H=28$ asteroid would have to be closer than 0.04 AU for its apparent magnitude to be equal to 21 mag. However, because of trailing losses, this object would have to be closer than 0.004 AU if its relative velocity were 9.5 km/s. Since volume scales as the third power of distance, a factor of 10 decrease in the distance translates into a factor 1,000 in the number of small bodies that this telescope would detect (assuming a uniform density distribution of small bodies).

We can now quantify the SNR variation among the three possible scenarios characterizing the strategy for detecting small and fast-moving NEAs:

1. One takes 2 long images separated in time, subtracts them and searches for a significant brightness deviations at the level of, say, 5σ . It is clear that since the NEA moves, its photons are spread out on the CCD in a streak over, say, 10 pixels (for a 10 sec exposure of $1''/\text{sec}$ motion and $1''$ pixel size). In this situation, peak detection only sees $1/10$ of the NEA photons. The SNR here is $1/10$ of that of a star (stationary object) of the same brightness.
2. Instead of looking for a peak in the difference of two images, one can attempt to use a matched filter to detect the streak. This method makes use of all of the photons from the NEA when the filter is a match to the actual streak. However, the larger area of the streak picks up more zodi background. The resulting SNR is $1/\sqrt{10}$ of that of a star of the same brightness. This method could be applied to traditional surveys but would be computationally intensive.
3. Finally, if we take short images over the same duration and then use a shift/add algorithm, we obtain the same SNR as for a star, which is a major advantage of the proposed method. In practical terms, for an NEA moving at $10^\circ/\text{day}$, the improvement of SNR with synthetic tracking, with a 30 sec exposure, would be ~ 12 -fold.

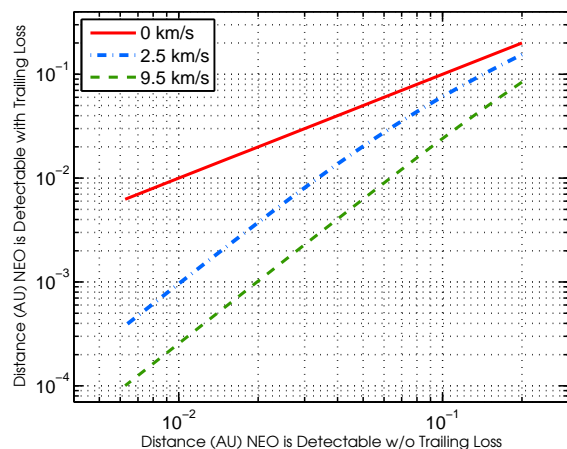


FIG. 4: The effect of trailing losses on the maximum detectable distance for NEAs of different H magnitude. Plotted is the maximum detectable distance with trailing loss vs. without trailing loss for three different relative velocities. All curves correspond to $V=21$ mag, the assumed sensitivity limit.

V. OBSERVATION OF ASTEROIDS 2013FQ10 AND 2009BL2

We tested the synthetic tracking approach using Caltech’s High-speed Multi-color camERA (CHIMERA) – a high-speed, two-color photometer, newly built for the prime focus of the Palomar 200-inch telescope.⁸ CHIMERA offers simultaneous observing in the Sloan g band, and either of the Sloan r or Sloan i bands. The instrument currently operates with a field of view (FOV) of $(2.5' \times 2.5')$, with a future upgrade underway to offer an larger range of filter choices and extend the FOV to $(8' \times 8')$. CHIMERA uses two AndorTM iXon 888 EMCCDs with (1024×1024) pixels, allowing high-speed (10 MHz readout) imaging in two colors with very low read noise ($< 1e^-$ with EM gain applied).

On Apr 3, 2013, we observed two known NEAs, 2013FQ10 and 2009BL2, taken from the JPL NEA list [8]. The data was taken with an AndorTM iXon camera at the prime focus of the Palomar 200-inch telescope, using the Winn corrector. A Sloan g' filter was in front of the CCD. The camera’s (512×512) pixels were binned (2×2) on chip, resulting in a (256×256) -pixel image with plate scale of $0.35''/\text{pixel}$. Data was recorded at 2 fps. The frames were time tagged with time from a GPS receiver, accurate to less than 1 msec. The results of observations of asteroid 2013FQ10 are shown in Fig. 5.

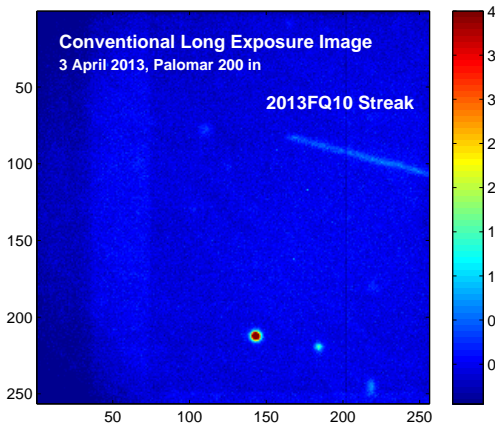


FIG. 5: NEA 2013FQ10 observed on April 3, 2013 at the Palomar 200 inch. 700 frames are added to form a conventional long exposure. The color map is adjusted to enhance the visibility of streak from the asteroid. A 19-mag star is prominent on the lower part of the image.

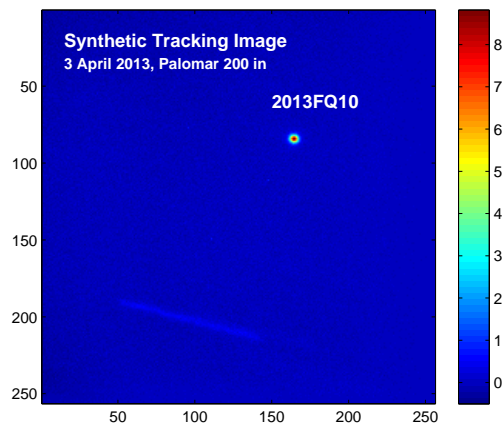


FIG. 6: NEA 2013FQ10 data processed according to the synthetic tracking approach. The asteroid now appears stationary while a faint streak is noticeable from the 19-mag star in the lower region.

2013FQ10 had an apparent magnitude of ~ 19.2 mag on April 3, 2013, with a velocity relative to the Earth of 9.2 km/s at a distance of ~ 0.12 AU. The proper motion of the asteroid is approximately $0.1''/\text{sec}$. We show 350 sec (700 frames) of data, discarding frames where the asteroid moved out of the field of view (FOV) of the camera. Fig. 5 shows the 700 frames co-added to create a conventional long exposure image. The streak from the asteroid is barely visible while the background shows a 19-mag star. The image uses a limited false color scale to highlight the asteroid. In this image, other background stars are visible and the 19-mag background star appears saturated. The brightness of the streak is ~ 10 – 20 times the noise background and read noise.

Fig. 6 shows the result of applying a simple shift/add algorithm. The SNR of 2013FQ10 in the shift/add image is about 400. Here SNR is defined as the asteroid flux divided by the 1σ noise in the background (excluding photon noise of the asteroid). Because in we used a shift vector to ‘freeze’ the asteroid, the 19-mag star is now a streak with degraded SNR.

The noise in the background is approximately 50% CCD read noise ($\sim 6e^-$) and 50% photon fluctuation in the zodi background. (In the future, we plan to switch to a second generation sCMOS camera that has $\sim 1e^-$ read noise, although slightly lower QE.) 2013FQ10 has a size of ~ 100 m (assuming an albedo of 12%). Had it been 14 m in diameter it would have been 23.4 mag and detected with a SNR of ~ 8 at a distance of 0.12 AU.

⁸ Caltech High-speed Multi-color camERA (CHIMERA): a prime focus instrument for the Palomar 200-inch telescope. PI: G. Hallinan; Instrument scientist: L. Harding, see details at <http://tauceti.caltech.edu/chimera/>.

NEA 2009BL2 is shown Figures 7 and 8. The first is from averaging the 1,000 frames to form a conventional image. The asteroid appears as a streak. The star peak pixel is 140 counts and appears saturated in this color map. The second image is formed using shift/add to remove the asteroid streak, resulting in an unsmeared spot for the asteroid, with a peak pixel of 15 counts. Again, the increase in SNR is visibly obvious as we synthetically track the asteroid. The asteroid is ~ 18.5 mag.

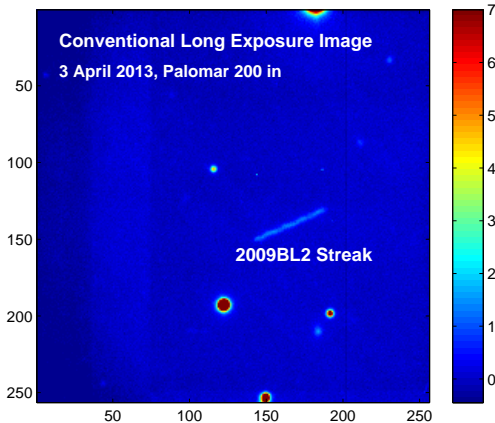


FIG. 7: NEA 2009BL2 observed on April 3, 2013 at the Palomar 200 inch. A conventional image is approximated by simply co-adding the frames.

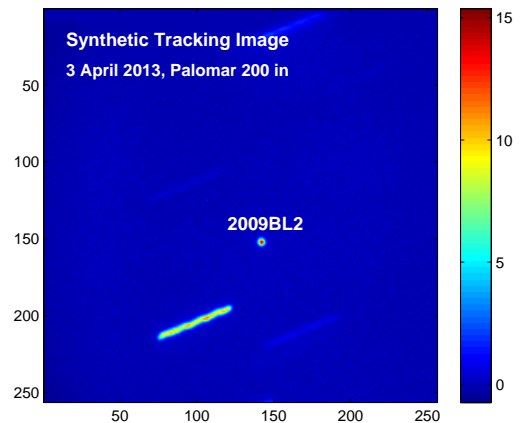


FIG. 8: NEA 2009BL2 observed on April 3, 2013 at the Palomar 200 inch. The image is from applying synthetic tracking to the short-exposure frames.

VI. ASTROMETRY

In the last 5 years, over 150 NEAs with $H \sim 28-30$ have been discovered, at a rate of ~ 30 such objects per year [8]. It is highly desirable to get the orbits of these objects with accuracy high enough that they will not be lost immediately after discovery. Many observatories that discover NEAs also conduct follow up observations of these objects. For bigger, ~ 100 m asteroids, the follow up astrometry can be done with telescopes other than the discovering telescope weeks or even months after discovery. With 30 discoveries of 10 meter-class NEAs per year, existing ‘follow up’ telescopes may be sufficient to get reasonable orbits. But if the discovery rate were to increase to 300 per year for small asteroids and a potentially much larger number for bigger (20–50 m class) asteroids, precise astrometry of a large number of targets may stress the existing suite of telescopes being used for follow up to get precise optical orbits.

As we shall describe below, astrometry at the 40 milliarcsecond (mas) level is the key to getting orbits with sufficient accuracy so those targets are properly identified at the next apparition. Synthetic tracking makes this level of accuracy by reducing the error in several ways. A synthetic tracking observatory may detect small fast moving asteroids that other observatories might find it hard to follow. Each observation of ~ 30 sec will measure the position and velocity of the object. For slow moving objects, a second observation ~ 30 min later will be needed to detect motion. Because each 30 sec synthetic tracking observation actually consists of many images, a very crude orbit can be derived from two observations at two epochs. This crude orbit can be used to plan the third epoch observation one or two days later. This third epoch might require up to ~ 300 sec measuring the position to ~ 30 mas. Approximately 3 or 4 of such 30 mas measurements over 1 month would be sufficient predict the position of the NEA at the next apparition to better than 1 arcmin.

Suggestion of the level of needed astrometric accuracy is from a simulation assuming a set of 4 astrometric measurements with ~ 40 mas accuracy and taken over approximately 2 months for an NEA in a near Earth-like orbit [3]. It was found that 40 mas would be sufficient to predict the NEA position to $\sim 10''$ at the next apparition 3–4 years in the future. This object would not be lost. For either faster or fainter objects that conventional CCD images could not detect, synthetic tracking would be needed and the discovering facility equipped with this technology would have to also do the follow up astrometric observations. If the initial detection were made by comparing two images roughly 30–60 min apart, the astrometry at each epoch would only be $\sim 0.1''$, limited by SNR. The astrometric follow-up to get to 30 mas would require ~ 300 sec of data. However, we would do this only for objects detected by the 2-epoch tracklet. Without any SNR penalty for rapid motion, we can detect NEAs of $H=28$ at a distance of ~ 0.044 AU or

~ 13 LD. If this object does not come within a few lunar distances of the Earth, there will be no radar data. It is also only observable for a couple of weeks at most.

A. Astrometric Errors

The present day optical astrometry of NEAs is much less accurate than the corresponding radar observations, sometimes by as much as 2–3 orders of magnitude. The state of the art in NEA astrometry is ~ 100 – 200 mas whereas ground-based stellar astrometry to measure parallaxes of nearby stars can be accurate to less than 1 mas [1]. There are many reasons for this accuracy discrepancy. One important reason is the star catalog. An asteroid search telescope can have a large field of view with a gigapixel focal plane composed of a mosaic of a large number of CCDs. But any astrometry of detected asteroids is limited to measuring the positions of stars within a single CCD. The spacing of the CCDs in a mosaic is neither accurate nor sufficiently stable for precision astrometry. Within the field of view of 1 CCD there are only a limited number of reference stars and this leads to lower astrometric accuracy.

The UCAC catalog published by the US Naval Observatory has 50 million stars down to ~ 16 mag [12]. Their positions are anchored to the stars in the Hipparcos and Tycho catalogs produced by the ESA Hipparcos mission, which operated in the early 1990's. The expected accuracy of the UCAC catalog is ~ 50 mas and is a major component of the ~ 100 – 200 mas error of asteroid astrometric observations. However, in October 2013, ESA will launch the Gaia astrometric satellite⁹ whose very first preliminary catalog (expected ~ 18 months later) will provide a reference frame better than 1 mas for objects down to ~ 19 – 20 mag. Once we combine our approach of detecting NEAs with astrometric data from the Gaia catalog, absolute astrometry of asteroids should improve by a factor of over a 100, from the current ~ 100 – 200 mas down to just a few mas.

B. Atmospheric Errors

In studying the data from the fast camera on Palomar, we identified an important source of astrometric error applicable to asteroid observations but not to stellar observations. It is well known that atmospheric turbulence can cause motion of the star by ~ 200 mas or more. Stellar astrometry can nonetheless be done at 1–3 mas because this atmospheric error is highly correlated ('common-mode') between the stars in the field. Most atmospheric turbulence is in the lower part of the atmosphere, where the resulting image motion is common to all the stars in the field. Differential motion is a result of turbulence at the top of the atmosphere, at altitudes of ~ 10 km, and is much smaller. The key to accurate differential astrometry is to make simultaneous measurements of the position of the target and reference stars. A time lag between the measurement of the target star and reference stars can result in much larger atmospheric errors. For a streaked asteroid image, the astrometric accuracy in the direction of the streak is obviously going to be worse than in the narrow direction of the streak. However, we believe a bigger effect of the streaked image is due to a non-simultaneity effect. In a 30 sec exposure, where the image is streaked by, say, $4''$, the initial quarter of the streak represents the first 7.5 sec and the final quarter of the streak the last 7.5 sec. For the reference stars, on the other hand, we have the average position over the entire 30 sec exposure.

We were able to test this hypothesis using our data on the asteroid 2013FQ10. We divided 600 frames data taken at 2 fps into 1-min segments and analyzed the data in two ways. In method 1, the frames within a 1 minute block were simply co-added to generate a conventional streaked image. In method 2, there were co-added using synthetic tracking. When the straight line motion of the asteroid is removed, the residuals are as shown in Fig. 9. Astrometric

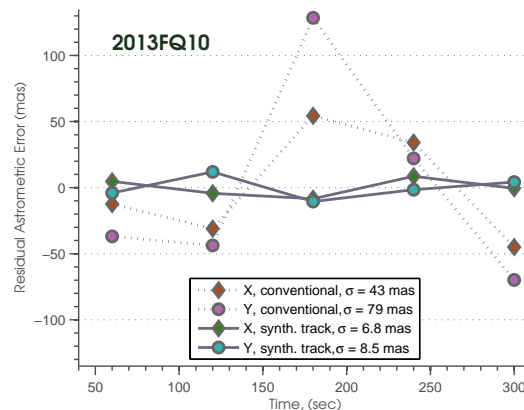


FIG. 9: For asteroid 2013FQ10 observed with the Palomar 200 inch telescope, the astrometric error is reduced from ~ 80 mas for the streaked image ('conventional') to 9 mas for the de-streaked image using synthetic tracking.

⁹ The ESA's Gaia mission's website: <http://sci.esa.int/gaia/>

residuals in the streaked image were ~ 80 mas in the direction of the streak, while the astrometric residuals were ~ 9 mas for the synthetically tracked images. Once the first Gaia catalog will be published, a few mas absolute astrometry of fast moving NEAs should be possible. The astrometric error in the streaked case is relatively low, under 100 mas, because the large aperture of the telescope averages over more atmosphere than a smaller telescope. A 1–2 m telescope searching for NEAs might expect 2–3 times larger atmospheric error, perhaps up to 200 mas for long streaked images.

In a subsequent paper [14] we will analyze the effect of non-simultaneity in more detail. Obviously if the streak is only $1.2''$ long, we would expect the astrometric precision to be close to a single digit milliarcsec precision of ground based stellar astronomers. However, NEAs are most often observed when they are closest to Earth. The loss of astrometric accuracy as a function of the length of the streak (in arcsec and seconds of time) will be explored and reported elsewhere. However our results on the asteroid 2013FQ10 show that the atmospheric error for a 1 minute measurement can be < 10 mas.

C. Photon Noise

For the smallest NEAs, however, the limiting factor in astrometric accuracy may not be atmospheric turbulence but photon noise. In general, the precision α of an astrometric measurement improves with the photometric SNR according to $\alpha = w/(2 \cdot \text{SNR})$, where w is the size of the spot or streak along the astrometric direction of interest. In photometric SNR, in contrast with detection SNR mentioned earlier, noise must also include the shot noise from the signal. For faint NEAs, synthetic tracking has higher photometric SNR because all the photons from the target are in a compact, seeing-limited image. As a result, for the fast moving ones synthetic tracking could detect objects normal CCD imaging cannot. It is useful to compare astrometric accuracy for an object that could be detected with normal CCD images with that from synthetic tracking. Consider an object that has a $(1'' \times 4'')$ streak (in a nominal 30 sec exposure) with the surface brightness of the streak equal to a star with SNR of 5. If we assume the astrometry analysis uses an optimal matched filter (e.g. an elongated Gaussian PSF) that also estimates the length and orientation of the streak, then all the signal photons would be used, enhancing the SNR roughly by the ratio $\sqrt{4''/1''}$. Along the streak, the noise-limited astrometric precision would then be $4''/(2 \cdot 5 \cdot \sqrt{4}) \sim 0.2''$. For synthetic tracking, on the other hand, the SNR for this example would be enhanced by a factor of about 4, to ~ 20 , so that the noise-limited astrometric precision would be $1''/(2 \cdot 20) \sim 0.025''$. For dim and fast moving objects, synthetic tracking offers a potential 8-fold improvement in astrometric precision, and this is not a small factor—it means reducing the required observation time by a factor of 64. For the smallest NEAs, astrometry of the ‘discovery’ images will be SNR limited to $\sim 0.1''$ – $0.07''$.

With synthetic tracking the noise-limited astrometric precision is better for two reasons, 1) the SNR is higher because all the NEA photons are in one spot and 2) the width of the image is the seeing width, with no streak. The SNR limited accuracy in this example would be $\sim 0.025''$ or over a factor of 8 better. In this example, we chose a NEA that was at the limit of detection for a normal CCD camera. A telescope with synthetic tracking camera could detect targets that could not be detected with a normal camera. If we now look at a smaller NEA one that is marginally detectable with synthetic tracking but not with a normal CCD camera, the astrometric precision would be $\sim w/(2 \cdot \text{SNR}) \sim 0.1''$ for an object that was about 4 times fainter. If we use our rule of thumb that astrometry at the 40 mas level is needed at nearly 4 epochs over the period of 2–3 months to get a NEA orbit with sufficient accuracy not to ‘lose’ it, then the follow up observations after initial detection should use integration times longer than 30 sec. If 30 sec gives a SNR limited accuracy of 100 mas, the follow up observations should be ~ 300 sec long to get to 30 mas accuracy. Note that from an SNR point of view, an eight times increase in accuracy implies increasing the integration time from 300 sec to $(64 \times 300 \text{ sec}) \sim 5$ hr. Such long integration times are not practical for astrometric follow up of NEA detections, especially if dozens of objects are detected every night.

D. Instrument Errors

The astrometric error of a measurement is not just due to SNR or the atmosphere. It is the RSS of both plus any instrumental errors. Because stellar parallax measurements have already demonstrated 1 mas accuracy, we expect that instrumental errors at the few milliarcsec level can be achieved. After the release of Gaia’s first catalog, the atmosphere and SNR will be the major contributing terms to errors of NEAs astrometry. If one adopts an observation cadence, with longer integration times to get to 30 mas accuracy, will this reduce the detection to discovery ratio from 100:1 to 1:1. We are currently conducting a relevant study, results of which will be reported elsewhere.

VII. DESIGN CONSIDERATIONS FOR A SMALL-NEA SEARCH INSTRUMENT

We now consider some general guiding principles in constructing an NEA search facility capable of searching the currently uncharted sub-100 meter NEA population, with particular attention to aspects relevant to a high-sensitivity instrument that employs synthetic tracking.

The ability of a telescope to survey large patches of the sky is given by its étendue [11]. Étendue is defined mathematically as the product of the light collecting area A and the (solid angular) field of view of the telescope Ω , or $(A \cdot \Omega)$. This quantity indicates the number of photons per unit frequency per unit time a telescope will accept, and is particularly important in conducting a large astronomical survey. For a wide variety of scientific investigations, one can trade solid angle for area. A larger area reduces integration time to reach a certain limiting magnitude but a small telescope with a large field of view can achieve the same performance as a larger one with a small field of view when the goal is to measure the brightness of every object. However, for some types of observations, one cannot substitute solid angle for area. If one is looking for millisecond variability of an object and the brightest object of that type is 18 mag, there is no substitute for a large collecting area. A search for small asteroids is an application where area and solid angle are not equivalent. For detection of small asteroids, the figure of merit is the volume of space in which certain sized objects can be detected per unit of time.

To illustrate, we compare two telescopes with the same étendue. The first is a 5 m telescope with a next Generation sCMOS ($4K \times 4K$) detector that has $FOV = 0.5^\circ$, and the second is a 1 m telescope with $FOV = 2.5^\circ$, and a CCD mosaic with ($20K \times 20K$) pixels (we assume the pixel sizes are the same in the two cases for simplicity). We can ask: “In a 30 sec observation, over what volume of space (in the anti-sun direction) could each of these two instruments detect an $H=28$ object that is moving with a transverse velocity of 10 km/s?” Had we been surveying for stars, the two would be equivalent; the smaller telescope could take 25 exposures, 30 sec each, to make up for the smaller collecting area, while the larger telescope would spend 30 sec looking at 25 different ($0.5^\circ \times 0.5^\circ$) parts of the sky. But there are additional considerations when looking for NEAs.

If we assume the limiting magnitude of the 1 m telescope is 21.3 mag, the corresponding limiting magnitude for the 5 m would be 23.0 mag for zodi-limited detection. For the 5 m telescope using synthetic tracking, there are no trailing losses and an $H = 28$ mag object can be detected at 0.1 AU. For the 1 m telescope with the larger CCD focal plane and using the basic technique, there would be a streak and trailing losses. As the NEA gets closer, the apparent magnitude will make the surface brightness of the streak increase faster than the lengthening of the streak makes it dimmer. At a distance of 0.005 AU, the surface brightness of the streak will be equal to a 21.3 mag star (the streak will be approximately $80''$ long). The volume of space searched by the two telescopes would compare as follows:

$$\begin{aligned} V_{5m} &= \frac{4\pi}{3} \cdot (0.1 \text{ AU})^3 \cdot \frac{(0.5 \text{ deg})^2}{41253 \text{ deg}^2} = 2.5 \times 10^{-8} \text{ AU}^3, \\ V_{1m} &= \frac{4\pi}{3} \cdot (0.005 \text{ AU})^3 \cdot \frac{(2.5 \text{ deg})^2}{41253 \text{ deg}^2} = 7.9 \times 10^{-11} \text{ AU}^3. \end{aligned} \quad (2)$$

The volume of space surveyed by the 5 m telescope with synthetic tracking is over 300 times larger, both systems having identical $(A \cdot \Omega)$.

In this example, we calculated the sensitivity loss according to Eq. (1). This assumes detection is possible only if the surface brightness of the streak is above the threshold for detecting a non-moving object. But algorithms specifically designed to detect streaks can find fainter objects. Nevertheless, this simple trailing loss of sensitivity formula allows us to predict how many NEAs with magnitudes of $H \sim 28-30$ can be detected with our reference 1-m telescope with limiting sensitivity of 21 mag with $FOV = 0.5^\circ$. Using the NEA population assumptions of Harris [5], we calculate that this strawman telescope operating 270 days per year, 8 hr per night should detect about 25 NEAs with $H \sim 28-30$ per year. This is roughly consistent with the ~ 30 such objects discovered per year with existing asteroid search telescopes.

Instead of comparing a 1-m telescope with a mosaic CCD, we could have hypothesized an sCMOS detector. The volume advantage is fundamentally due to the fact the sCMOS detector equally high sensitivity for fast moving objects. However, sCMOS detectors cannot be efficiently packed into a mosaic. A normal CCD is mostly photosensitive area and the readout electronics on the chip occupies an area that is very small compared to photosensitive area. This is not true for current sCMOS detectors; the silicon around the photosensitive area is fully utilized and necessary to achieve the high speed readout at the very low noise of these detectors. If the 1 m telescope were to convert to a single sCMOS camera and employ synthetic tracking, the distance out to which the $H = 28$ mag object would be detectable by it would increase to 0.045 AU, and the searchable-volume advantage of the 5 m would shrink down to a factor of about 11. There are expected to be ~ 100 million near Earth objects at $H \sim 28-30$ mag. A 1 m telescope with a $FOV = 1 \text{ deg}^2$ could potentially detect 10–20 such objects in one night, out to a distance of 0.045 AU.

Étendue can also be viewed as the product of the telescope area and the focal plane area. If we cannot increase the focal plane area by mosaicking detectors, the most sensitive instrument for detecting the smallest ($H \sim 28-30$) NEAs is the biggest detector on the biggest telescope. In a hypothetical next generation sCMOS camera, on the Palomar 200-inch, the field corrector lens would have a focal ratio $f/1.2$ onto a backside-illuminated sCMOS detector with $16 \mu\text{m}$ pixels. With $16 \mu\text{m}$ pixels, it is not possible to efficiently use a telescope larger than 5 m. Thus, the optimal next-generation facility employing synthetic tracking would be a 5 m telescope with an $f/1.2$ field corrector and a single, backside illuminated sCMOS detector.

VIII. CONCLUSIONS

Large near-Earth asteroids 250 m in diameter can be detected 0.25 AU from the Earth and their motion across the sky can be slow enough that ~ 30 sec CCD exposures only result in short streaks. However, an NEA 10 times smaller in diameter has to come 10 times closer to Earth to be detected and on average it will be moving 10 times faster across the sky. As the NEA moves faster across the sky, the sensitivity of conventional 30 sec CCD exposures decreases. Trailing losses the loss of sensitivity from a streaked image, while not very serious for 250 m NEA is a major factor for 10 m sized NEAs. In this paper we describe a new type of camera and data processing approach that can detect fast moving small NEAs with essentially no loss of sensitivity due to trailing losses. Such a camera on a large 5 m telescope should be able to discover ~ 80 NEAs of $H \sim 28-30$ in one night, the rate which almost 1000 times higher than the discovery rate of these small objects over the last 5 years.

The other advantage of synthetic tracking is significantly higher astrometric accuracy of NEAs. Narrow angle astrometry with $\sim 5-10$ mas accuracy coupled with a catalog of reference stars from the GAIA mission should mean that observation of even 10 m NEA at $\sim 3-4$ epochs over a few days would be sufficient to measure the orbit so these objects are not subsequently lost. Last, milliarcsec level astrometry will enable astronomers to measure the area/mass ratio of all asteroids, and when their physical size is measured with radar or thermal IR photometry, one can calculate the masses of these NEAs.

Acknowledgments

The authors wish to thank Dr. J. Giorgini of JPL for the simulation of what astrometric accuracy is needed to “not lose” an asteroid in a near earth orbit, and Dr. P. Chodas of JPL for supplying the estimates for the NEA population in the range of magnitudes $H \sim 26-31$. We also thank Prof. V. E. Zharov of the Lomonosov Moscow State University for useful comments on the manuscript. The work described here was carried out at the Jet Propulsion Laboratory, California Institute of Technology, under a contract with the National Aeronautics and Space Administration. Government sponsorship acknowledged. Copyright 2013 California Institute of Technology.

-
- [1] Boss A. P. et al., 2009, PASP, 121, 1218
 - [2] Chodas, P., 2013, private communication, JPL
 - [3] Giorgini, J., 2013, private communication, JPL
 - [4] Gural, P. S., Larsen, J. A., Gleason, A. E., 1985, AJ, 130, 1951
 - [5] Harris, A., 2011, presentation at the TARGET NEO Workshop, George Washington University, February 22, 2011, <http://targetneo.jhuapl.edu/pdfs/sessions/TargetNEO-Session2-Harris.pdf>
 - [6] Kubica, J., Denneau, L., Grav, N., Heasley, J., Jedicke, R., Masiero, J., Milani, A., Moore, A., Tholen, D., Wainscoat, R. J. 2007, Icarus 189, 151
 - [7] NASA NEO Report 2007, “Near-Earth Object Survey and Deflection,” Report to Congress, http://www.nasa.gov/pdf/171331main_NEO_report_march07.pdf
 - [8] NEO program website 2013, <http://neo.jpl.nasa.gov/stats/>
 - [9] NRC report Defending Planet Earth: Near-Earth Object Surveys and Hazard Mitigation, 2010, National Academies Press, ISBN 0-309-14969
 - [10] Stokes, G. H., et al. 2003, Report of the Near-Earth Object Science Definition Team, Prepared at the Request of NASA Office of Space Science Solar System Exploration Division, <http://neo.jpl.nasa.gov/eo/neoreport030825.pdf>
 - [11] Tonry, J. L., 2009, PASP, 123, 58
 - [12] USNO CCD Astrograph Catalog(UCAC) <http://www.usno.navy.mil/USNO/astrometry/optical-IR-prod/ucac>
 - [13] Vereš, P., et al., 2012, PASP, 124, 1197
 - [14] Zhai, C., et al., 2013, in preparation.